

**Study of Co-optimization Stochastic SuperOPF  
Application in  
the CAISO System**

Supplementary Report

Prepared for

Prepared by  
Bigwood Systems, Inc.  
Ithaca, NY

June 2015

# Table of Contents

1. Data Preparation.....	4
2. Simulation Settings.....	8
2.1 The test system.....	8
2.2 Hardware and software.....	8
2.3 Optimization variables .....	9
2.4 Stopping criteria .....	9
3. Simulation Results .....	10
3.1 CPFLOW Computation .....	10
3.2 Basecase Optimization under Different Loading Conditions.....	11
3.3 Worst Contingencies and Post-Contingency Optimization.....	15
3.4 Base-case + Individual Contingency Co-optimization .....	19
3.5 Base-case + All Contingency Co-optimization .....	22
4. Summary.....	26

## List of Figures

Figure 1-1: Illustration of piece-wise cost model.....	6
Figure 1-2: Illustration of the proxy variable for piece-wise costs.....	6
Figure 3-1: P-V curves for selected buses (500KV, voltage drop greater than 0.15p.u.)..	10
Figure 3-2: Basecase loss minimization under different loading conditions.....	12
Figure 3-3: Basecase cost minimization under different loading conditions .....	15
Figure 3-4: Post-contingency loss minimization under different loading conditions .....	18
Figure 3-5: Post-contingency cost minimization under different loading conditions .....	19
Figure 3-6: “Basecase + single-contingency” co-optimization for loss minimization.....	20
Figure 3-7: “Basecase + single-contingency” co-optimization for cost minimization .....	22
Figure 3-8: Summarized loss minimization results.....	25
Figure 3-9: Summarized cost minimization results .....	25

## List of Tables

Table 1-1: The PSSE data header.....	4
Table 1-2: The monitor list file.....	4
Table 1-3: The levelized cost of electricity (LCOE) for different generation resources .....	5
Table 3-1: Loading conditions for simulation .....	10
Table 3-2: Basecase loss minimization under different loading conditions .....	11
Table 3-3: Convergence for basecase cost minimization .....	14
Table 3-4: Basecase cost minimization under different loading conditions .....	14
Table 3-5: Worst “N-1” contingencies.....	15
Table 3-6: Convergence for post-contingency optimization.....	16
Table 3-7: Post-contingency loss minimization under different loading conditions .....	17
Table 3-8: Post-contingency cost minimization under different loading conditions .....	18
Table 3-9: Convergence for “basecase + single-contingency” co-optimization .....	19
Table 3-10: “Basecase + single-contingency” co-optimization for loss minimization .....	20
Table 3-11: “Basecase + single-contingency” co-optimization for cost minimization .....	21
Table 3-12: Convergence for “basecase + all-contingency” co-optimization .....	23
Table 3-13: “Basecase + all-contingency” co-optimization .....	24

# 1. Data Preparation

This supplementary report creates a new CAISO system dataset and presents SuperOPF simulation results on the dataset. The dataset is configured based on a recent BSI VSA study case for CAISO. The data header for the PSSE raw data file is shown in Table 1-1.

Table 1-1: The PSSE data header

0	100.0	/	PSS/E-30.0	BY	BSI	VSA
S=DB62_Version_VSA_H_STATIC_011613.xml		D=CIM_periodic_070213_033022.xml				
Create on 03/10/15 11:20:03						

The same loading pattern used in BSI VSA study is used to generate CPFLOW solutions under different loading conditions. These CPFLOW solutions will be used as initial conditions for SuperOPF computations. It is known that there is no bus voltage limits specified in PSSE raw data files. In creating the dataset, bus voltage limits are retrieved from the monitor list file of VSA study. A portion of the monitor list file is shown in Table 1-2, which also illustrates the structure of the file. The monitor voltage range for a bus specified in the file is used as the valid range of voltage magnitude for the bus in SuperOPF computations; for other buses not covered in the monitor list file, a generic range of [0.9, 1.1] is used as the bus voltage range for SuperOPF computation. As shown in Table 1-2, it is also specified in the monitor list file are the monitored branches. For branches included in the monitor list file, thermal limit constraints will be imposed for SuperOPF computation; no thermal limit constraints will be considered for other branches. The RateA value for branches specified in the PSSE raw data file will be used as the thermal limits in SuperOPF computation.

Table 1-2: The monitor list file

MONITOR BRANCHES							
35901	14	1	/* MRGHLJ-GRNVLY_115_BR_2_1				
...	...	...					
END							
MONITOR VOLTAGE RANGE	BUS	18972	0.9500	1.0500	/* COPMT2		1-BUS-230
MONITOR VOLTAGE DEVIATION	BUS	18972	0.0500	0.0500	/* COPMT2		1-BUS-230
MONITOR VOLTAGE RANGE	BUS	18974	0.9522	1.0507	/* COPMT2		1-BUS-34.5
MONITOR VOLTAGE DEVIATION	BUS	18974	0.0500	0.0500	/* COPMT2		1-BUS-34.5
...	...	...					
END							

Table 1-3: The levelized cost of electricity (LCOE) for different generation resources <sup>1</sup>

Plant Type	Range for Total System LCOE (2012 \$/MWh)			Range for Total LCOE with Subsidies <sup>1</sup> (2012 \$/MWh)		
	Minimum	Average	Maximum	Minimum	Average	Maximum
<b>Dispatchable Technologies</b>						
Conventional Coal	87.0	95.6	114.4			
IGCC	106.4	115.9	131.5			
IGCC with CCS	137.3	147.4	163.3			
<b>Natural Gas-fired</b>						
Conventional Combined Cycle	61.1	66.3	75.8			
Advanced Combined Cycle	59.6	64.4	73.6			
Advanced CC with CCS	85.5	91.3	105.0			
Conventional Combustion Turbine	106.0	128.4	149.4			
Advanced Combustion Turbine	96.9	103.8	119.8			
Advanced Nuclear	92.6	96.1	102.0	82.6	86.1	92.0
Geothermal	46.2	47.9	50.3	43.1	44.5	46.4
Biomass	92.3	102.6	122.9			
<b>Non-Dispatchable Technologies</b>						
Wind	71.3	80.3	90.3			
Wind – Offshore	168.7	204.1	271.0			
Solar PV <sup>2</sup>	101.4	130.0	200.9	92.6	118.6	182.6
Solar Thermal	176.8	243.1	388.0	162.6	223.6	356.7
Hydroelectric <sup>3</sup>	61.6	84.5	137.7			

The generation cost data is created based on several data sources. The levelized cost of electricity (LCOE) for different generation resources, as shown in Table 1-3, is used as the reference for generating the generation costs. The generation types are retrieved from QFER CEC-1304 Power Plant Owner Reporting Database published by California Energy Commission <sup>2</sup>. Generator names are matched to the generator bus names recorded in the PSSE raw data file. Two types of costs are assigned to the generators, namely, linear and piece-wise linear costs. The cost values are drawn randomly following uniform distribution from the range of the LCOE shown in Table 1-3. Figure 1-1 illustrates the piece-wise linear cost model. Piece-wise linear costs are assigned to 10% of the total number of generators, each has 2 to 5 cost segments in the range of the minimal and maximal generations; other generators are assigned with linear costs.

<sup>1</sup> Levelized Cost and Levelized Avoided Cost of New Generation Resources in the Annual Energy Outlook 2014, U.S. Energy Information Administration.

<sup>2</sup> [http://www.energyalmanac.ca.gov/electricity/web\\_qfer/source\\_files/q\\_WebWorks\\_QFERPlant\\_Table.txt](http://www.energyalmanac.ca.gov/electricity/web_qfer/source_files/q_WebWorks_QFERPlant_Table.txt).

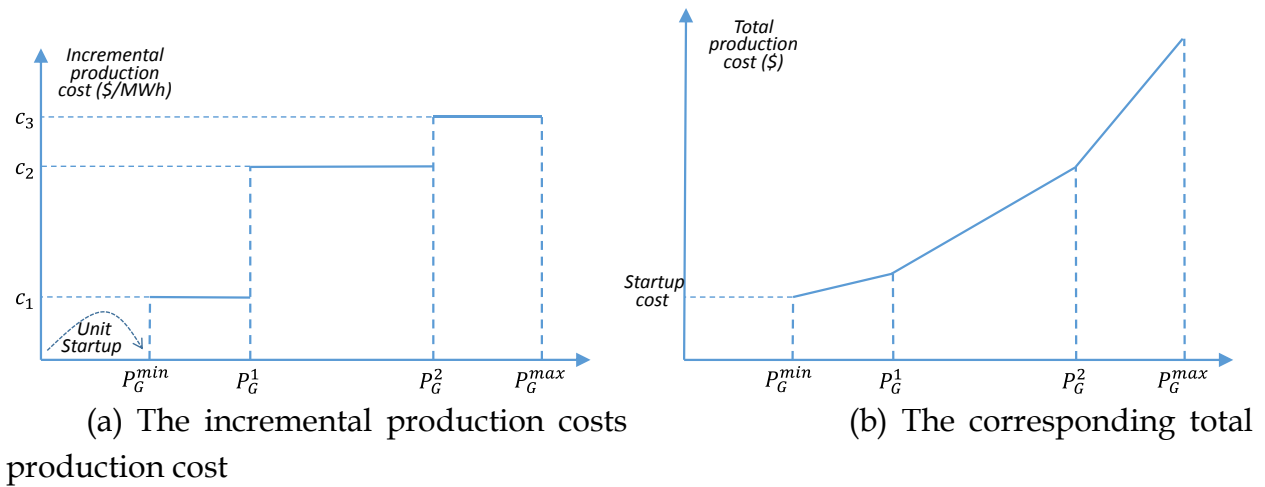


Figure 1-1: Illustration of piece-wise cost model

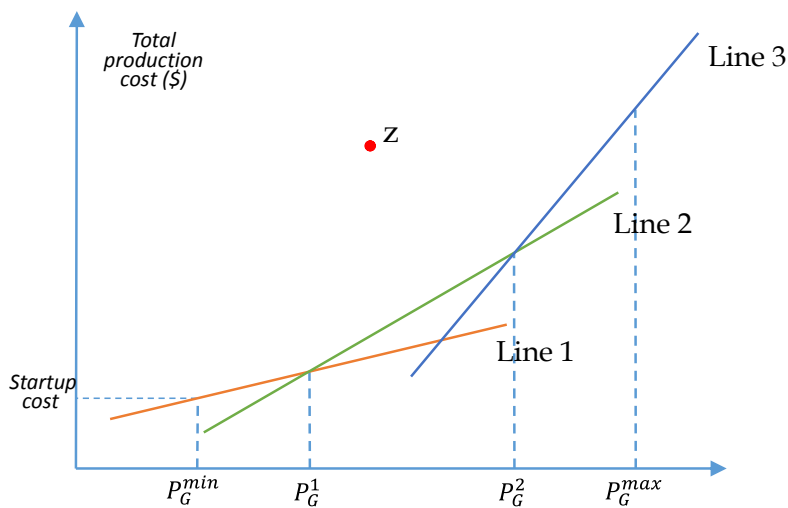


Figure 1-2: Illustration of the proxy variable for piece-wise costs

Figure 1-2 illustrates the technique for handling piece-wise linear costs. Basically, a proxy cost variable, noted as  $z_i$  for  $i$ -th generator with piece-wise linear cost, is added to the OPF problem formulation, along with the following new set of proxy constraints

$$\begin{aligned}
 z_i &\geq a_{1i}P_i + b_{1i} \\
 z_i &\geq a_{2i}P_i + b_{2i}, \\
 &\dots \dots \\
 z_i &\geq a_{Ki}P_i + b_{Ki}
 \end{aligned}$$

where,  $K$  is the number of cost segments,  $a_{1i}, \dots, a_{Ki}$  and  $b_{1i}, \dots, b_{Ki}$  are the cost parameters for the lines of the cost segments.

## 2. Simulation Settings

### 2.1 The test system

The test system is a CAISO 7199-bus VSA study case, of the following dimensions:

- Number of buses: 7199
- Number of loads: 3004
- Number of generators: 2097
- Number of non-transformer branches: 6551
- Number of transformers: 2533
- Number of switched shunts: 579
- Basecase System load:  $76323.36\text{MW} + j 9872.40\text{MVar}$

### 2.2 Simulation Targets

Two types of objective functions are considered in the simulation, including

- To minimize the system real power losses, and
- To minimize the system production costs.

Co-optimization is carried out for worst “N-1” contingencies. All computations will be carried out under different loading conditions.

In this simulation, for co-optimization with reserves, the generator(s) at the slack bus(es) is treated as the reserve source. In other words, the remainder generation capability of the slack generator(s) will be considered as available up-spinning reserve for contingency scenarios. Therefore, in the resultant OPF solutions, all non-slack generators will have same outputs across all involved contingencies.

### 2.3 Hardware and software

All the simulations in this report have been carried out on a personal computer with the following configuration:

- CPU: Intel Core i7-3820QM Quad 2.70GHz (Turbo Boost up to 3.7 GHz) with 8MB shared L3 cache
- Memory: 16GB 1600MHz DDR3L SDRAM
- Storage: 512GB Flash Storage Drive
- OS: Ubuntu Linux 15.04 AMD64, Linux Kernel 3.19.0, GCC5.1.1
- Software: BSI SuperOPF v3.90

## 2.4 Optimization variables

In the simulations, the following categories of optimization variables are adjusted by SuperOPF in the OPF computations:

- $V_m$ : Bus voltage magnitudes.
- $V_a$ : Bus voltage phase angles.
- $P_g$ : Generator real power outputs.
- $Q_g$ : Generator reactive power outputs.
- $t$ : ULTC transformer tap ratios.
- $s$ : phase shifters.
- $b$ : switchable shunts.

## 2.5 Stopping criteria

For the involved simulations, the stopping criteria for the OPF computation by BSI SuperOPF are specified as follows:

- The maximum allowable iterations: 500.
- The convergence tolerance for P-mismatches is 0.01MW.
- The convergence tolerance for Q-mismatches is 0.1MVar.
- The convergence tolerance for thermal limits is 0.01MVA.
- The convergence tolerance for voltage magnitude bounds is  $1e-4$  p.u.
- The convergence tolerance for shunt device bounds is 0.01MVar.
- The convergence tolerance for transformer tap ratio bounds is  $1e-4$ .
- The convergence tolerance for phase shifter phase angle bounds is  $1e-4$  rad.

### 3. Simulation Results

#### 3.1 CPFLOW Computation

In this simulation, in order to obtain power flow solutions under different loading conditions, BSI’s voltage stability analysis (VSA) program is used to perform a CPFLOW computation on the test system. The “SDGE+CFE-BG-LOAD\_INC” loading pattern is simulated, that is, loads are increased only in area 11 “SDGE-22” and power flow solutions are computed until the nose point of the P-V curves is reached, beyond which no power flow solutions exist.

Table 3-1: Loading conditions for simulation

Case	1	2	3	4	5	6	7	8
Load (MW)	76323.36	76489.11	77024.66	77541.53	78044.94	78532.81	78972.60	79052.42
Violations	#V: 41	#V: 41	#V: 37	#V: 42	#V: 49	#V: 49	#V: 180 #T: 1	#V: 215 #T: 1

Basecase system load margin: 2738.8MW. (“#V” for the number of voltage magnitude violations, “#T” for the number of thermal limit violations)

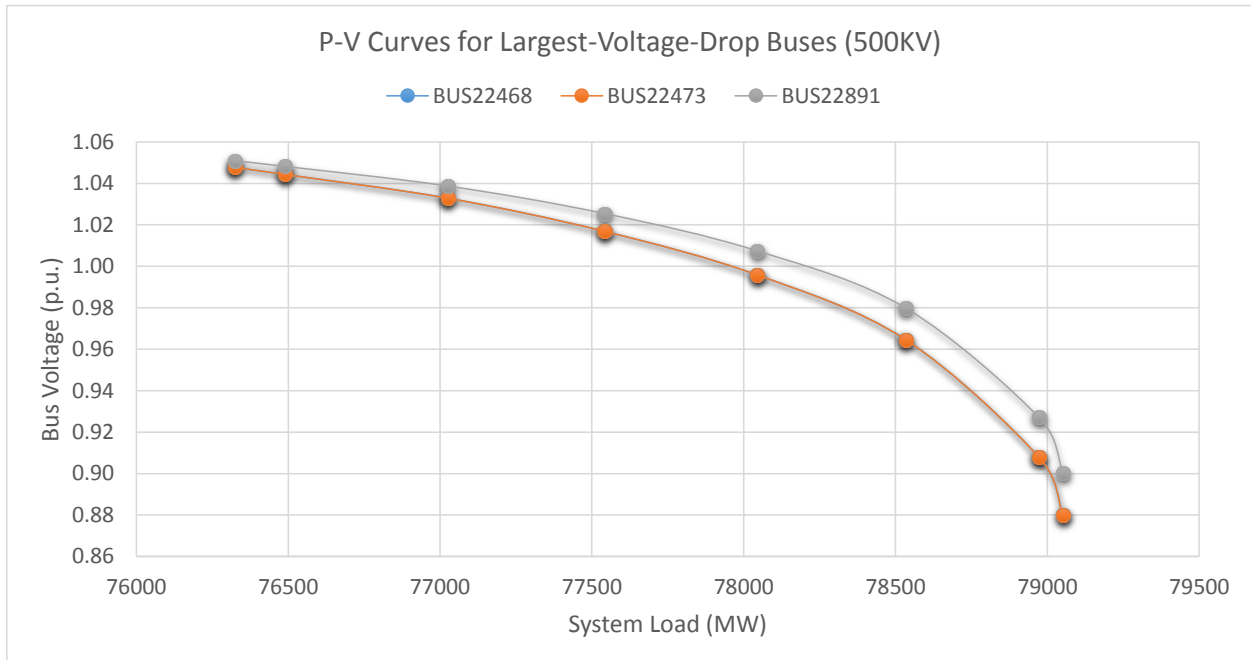


Figure 3-1: P-V curves for selected buses (500KV, voltage drop greater than 0.15p.u.)

There are eight points on the P-V curves, starting from the base load until the nose point, obtained by VSA CPFLOW computation, as summarized in Table 3-1 and depicted in Figure 3-1. These power flow solutions are used as the initial conditions for OPF computation. It needs to be noted that although these points correspond to power flow solutions under different loading conditions, they can still have violations, therefore are not feasible solutions to the OPF problem, as also shown in Table 3-1.

### 3.2 Basecase Optimization under Different Loading Conditions

The first simulation is to use SuperOPF to perform system power loss and production cost minimization on the basecase system under different loading conditions.

Table 3-2: Basecase loss minimization under different loading conditions

Case	Load (MW)	PLoss0 (MW)	PLoss1 (MW)	Reduction	Iters	Time
1	76323.36	2672.63 (3.502%)	1420.40 (1.861%)	46.85%	77	7.95
2	76489.11	2684.16 (3.509%)	1423.96 (1.862%)	46.95%	149	15.47
3	77024.66	2726.84 (3.540%)	1438.40 (1.867%)	47.25%	96	10.07
4	77541.53	2784.84 (3.591%)	1456.76 (1.879%)	47.69%	82	8.51
5	78044.94	2859.73 (3.664%)	1479.10 (1.895%)	48.28%	45	4.67
6	78532.81	2957.29 (3.766%)	1526.84 (1.944%)	48.37%	84	8.69
7	78972.60	3091.82 (3.915%)	No OPF solution (problem infeasible)			
8	79052.42	3137.98 (3.969%)	No OPF solution (problem infeasible)			

The results on system power loss minimization are summarized in Table 3-2 and Figure 3-2. In the results,

- PLoss0: the CPFLOW solution losses and
- PLoss1: the OPF solution losses.

Following observations can be drawn from the results:

- The two largest loading conditions result infeasible OPF problems. We can have a visual inspection from Figure 3-1, which also provides some clue about this, since for these two largest loading conditions, in order to meet the demands, the selected bus voltage magnitudes have to drop below their lower bounds (0.95 p.u. for bus 22891, 0.9 p.u. for buses 22468 and 22473).
- The infeasibility of the two largest loading conditions is formally validated with our feasibility analysis engine. This engine transforms the task of finding feasible points to the OPF problem into the task of computing stable equilibrium points (SEPs) and stable equilibrium manifolds (SEM) in a tailored dynamical system. The findings is summarized in Table 3-3, which reveals that, for both loading conditions, there is no SEMs found that correspond to feasible regions, while only one null space SEP is found with non-zero energy value. The null space SEP is in fact the point in the search domain that is closest to be feasible.
- The SuperOPF solver can robustly compute the OPF solutions under all feasible loading conditions.
- SuperOPF can effectively reduce almost half system losses under all loading conditions, and the reduction rate tends to increase as system loads increase.
- The OPF system losses (percentage with respect to the system load) increase as system loads increase, but with lower rates than that of CPFLOW solutions. Both rates are higher than the increasing rate of the system total loads. In a word, such changes are nonlinear.

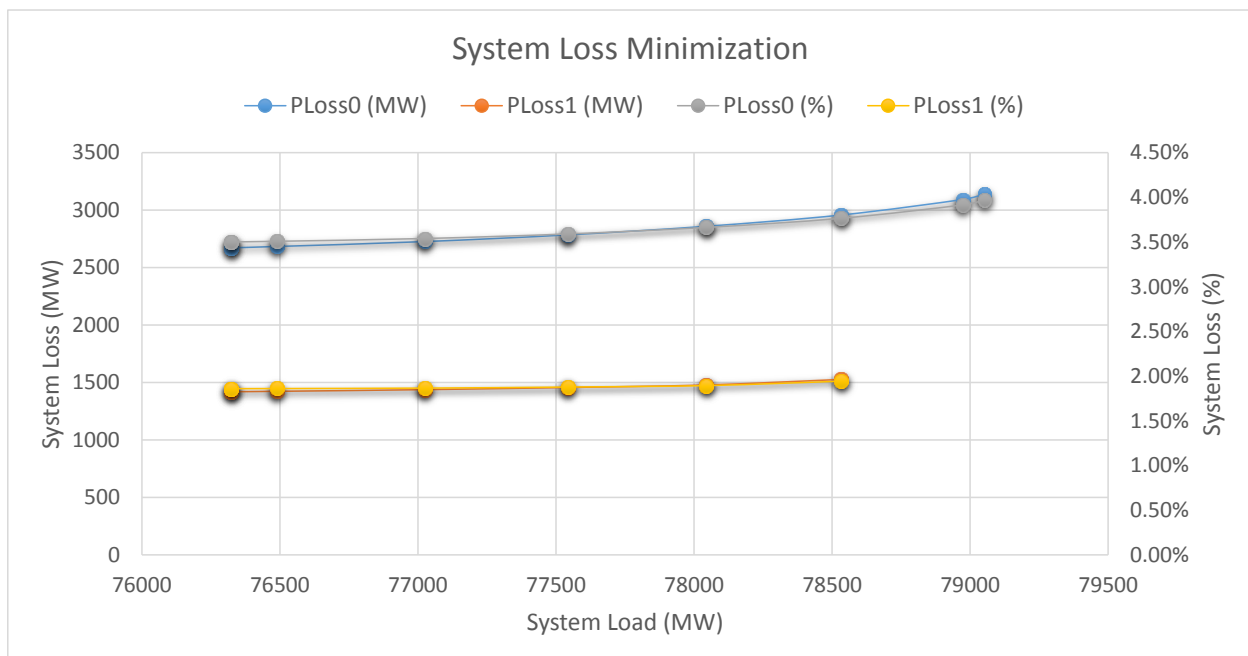


Figure 3-2: Basecase loss minimization under different loading conditions

Table 3-3: Infeasibility validation for the two largest loading conditions

Case	SEM	SEP	SEP Energy	Violations for SEP
7	None	1	$2.92 \times 10^{-4}$	Six voltages with violations greater 0.001 p.u. , which the largest being 0.0114 p.u.
8	None	1	$3.91 \times 10^{-4}$	Seven voltages with violations greater 0.001 p.u., which the largest being 0.0124 p.u.

The results on system production cost minimization are summarized in Table 3-4, Table 3-5 and Figure 3-3. In the results,

- PCost0: the CPFLOW solution costs and
- PCost1: the OPF solution costs.

Following observations can be drawn from the results:

- Table 3-4 summarizes the convergence of the computation under different loading conditions. It can be seen that conventional IPM cannot converges for all loading conditions; more specifically, it failed to converge for four among six feasible cases. In contrast, for these non-convergent cases, our SuperOPF solution method can still successfully converge to the desired OPF solutions.
- Therefore, SuperOPF solver can still robustly compute the OPF solutions under all feasible loading conditions.
- As shown in Table 3-5, SuperOPF can effectively reduce more than 12% system production costs under all loading conditions. Although this is achieved on the synthetic cost data, it is still reasonable to expect the significant economic impact brought by SuperOPF for real-life production cost data.
- As also shown in Table 3-5, the rate of OPF system production cost reduction (the costs of OPF solution with respect to that of the initial power flow solutions) tends to decrease as system loading condition becomes heavier.
- As shown in Figure 3-3, the change of the production costs is almost linear with respect to the change of system loads. This is because that the majority of the generators is assigned a linear cost, while only about 10% of the generators are assigned a piece-wise linear cost.

Table 3-4: Convergence for basecase cost minimization

Case	Load (MW)	IPM	SuperOPF
1	76323.36	Failed	Converged
2	76489.11	Converged	Converged
3	77024.66	Failed	Converged
4	77541.53	Failed	Converged
5	78044.94	Converged	Converged
6	78532.81	Failed	Converged
7	78972.60	No OPF solution (problem infeasible)	
8	79052.42	No OPF solution (problem infeasible)	

Table 3-5: Basecase cost minimization under different loading conditions

Case	Load (MW)	PCost0 (\$/Hr)	PCost1 (\$/Hr)	Reduction	Iters	Time
1	76323.36	8695662.83	7582236.18	12.80%	59	8.58
2	76489.11	8715101.45	7598383.37	12.81%	45	7.20
3	77024.66	8778607.18	7668672.15	12.64%	67	9.55
4	77541.53	8841738.16	7719517.58	12.69%	43	7.00
5	78044.94	8905250.95	7777127.93	12.67%	42	7.49
6	78532.81	8969524.78	7836365.40	12.63%	76	10.55
7	78972.60	9032534.30	No OPF solution (problem infeasible)			
8	79052.42	9046363.55	No OPF solution (problem infeasible)			

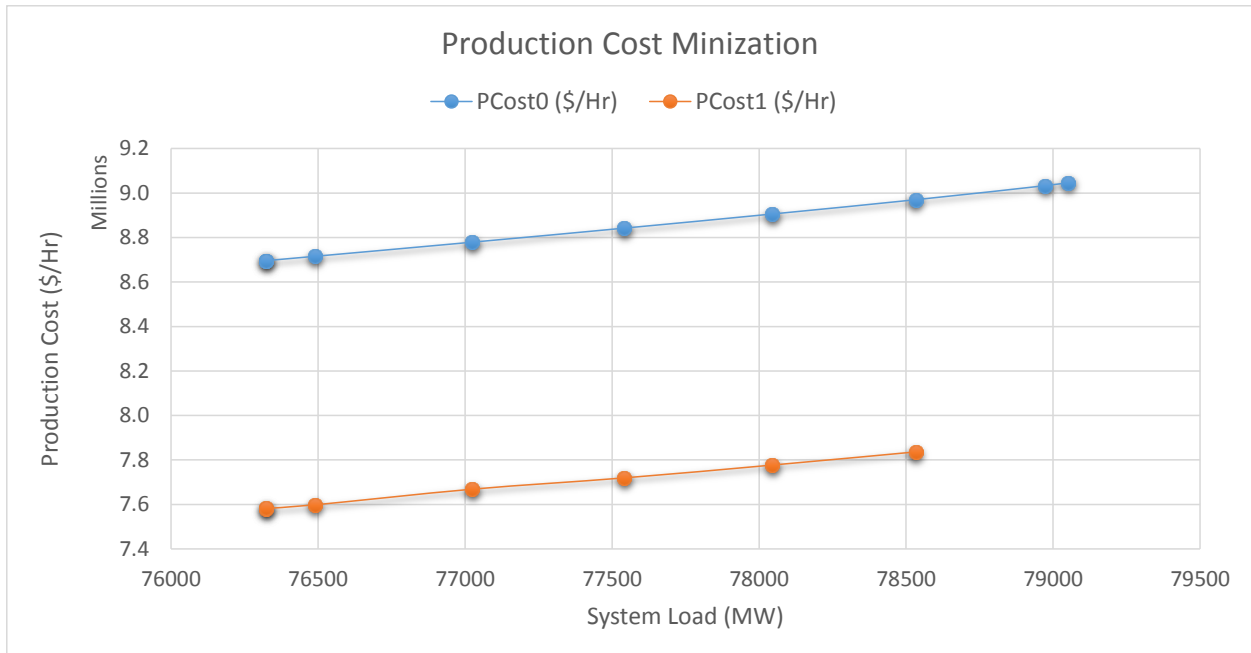


Figure 3-3: Basecase cost minimization under different loading conditions

### 3.3 Worst Contingencies and Post-Contingency Optimization

In this simulation, “N-1” transmission line contingencies are first generated by BSI VSA program, then BSI VSA is used to estimate load margins for the post-contingency systems. Contingencies are ranked in terms of their margins and worst contingencies are identified as those ones with least load margins. There are two “N-1” transmission line contingencies identified by BSI VSA, which have zero load margins; in other words, these contingencies are insecure in that the system cannot support the system load demands should any of these contingencies happen. The details of these two worst contingencies are summarized in Table 3-6.

Table 3-6: Worst “N-1” contingencies

Ctg ID	Details	Load Margin
0	Basecase	2738.8MW
558	DISCONNECT BRANCH FROM BUS 11217 TO BUS 11093 CKT 1 /* AFTON-LUNA 345.0 KV Line	0MW

2909	DISCONNECT BRANCH FROM BUS 34774 TO BUS 34776 CKT 1 /* MIDWAY-TAFT 115.0 KV Line	0MW
------	---	-----

Table 3-7: Convergence for post-contingency optimization

Case	Load (MW)	IPM				SuperOPF
		Loss Minimization		Cost Minimization		
		Ctg_558	Ctg_2909	Ctg_558	Ctg_2909	
1	76323.36	Converged	Converged	Converged	Converged	Converged
2	76489.11	Converged	Failed	Converged	Converged	Converged
3	77024.66	Converged	Converged	Failed	Failed	Converged
4	77541.53	Converged	Converged	Converged	Converged	Converged
5	78044.94	Converged	Converged	Converged	Failed	Converged
6	78532.81	Failed	Failed	Failed	Converged	Converged

Table 3-7 summarizes the convergence of OPF computation for the post-contingency systems under different loading conditions. It can be seen that conventional IPM cannot converge for all post-contingency loading conditions; more specifically, it failed to converge for seven among 24 cases. In contrast, our SuperOPF solver is able to successfully converge to the desired OPF solutions for both worst contingencies under all loading conditions.

The results on post-contingency power loss minimization are summarized in Table 3-8 and Figure 3-4. In the results,

- PLoss1: the basecase OPF solution losses,
- PLoss2: the post-contingency-558 OPF solution losses, and
- PLoss3: the post-contingency-2909 OPF solution losses.

Following observations can be drawn from the results:

- SuperOPF can robustly compute the OPF solutions under all feasible loading conditions, even though the post-contingency systems are insecure. This is due to more controllable generations available for OPF computation, instead of the single slack generator for power flow computation (though other generations are changed before computation to support the load demand).

- Since only one transmission line is taken out in the “N-1” contingencies, its impact on the resulted post-contingency system losses is not significant. As shown in Table 3-8, the variations of the post-contingency OPF losses across are less than 2% with respect to the basecase OPF losses.
- It can also be observed that, contingencies do not necessarily always increase the OPF losses. As shown in Table 3-8, compared to the basecase system OPF losses shown in Table 3-2, contingency #558 consistently increases the post-contingency OPF losses under all loading conditions. In contrast, contingency #2909 introduces almost not impact on the OPF losses for loading conditions 1 through 5; for the loading condition 6, it can result better loss reduction compared to the basecase OPF. This is related to another interesting research topic of optimal line switching for different purposes, such as system loss reduction and transfer capability improvement.

Table 3-8: Post-contingency loss minimization under different loading conditions

Case	Load (MW)	Ctg_558			Ctg_2909		
		P <sub>Loss2</sub> (MW)	Iters	Time (s)	P <sub>Loss3</sub> (MW)	Iters	Time (s)
1	76323.36	1446.84 (1.896%)	168	17.57	1420.50 (1.861%)	80	8.40
2	76489.11	1450.42 (1.896%)	160	17.12	1423.95 (1.862%)	83	12.86
3	77024.66	1465.40 (1.903%)	176	18.26	1438.36 (1.867%)	138	14.55
4	77541.53	1482.84 (1.912%)	81	8.34	1456.80 (1.879%)	107	11.56
5	78044.94	1505.67 (1.929%)	169	17.45	1479.10 (1.895%)	84	8.75
6	78532.81	1546.86 (1.970%)	101	14.33	1521.26 (1.937%)	50	9.34

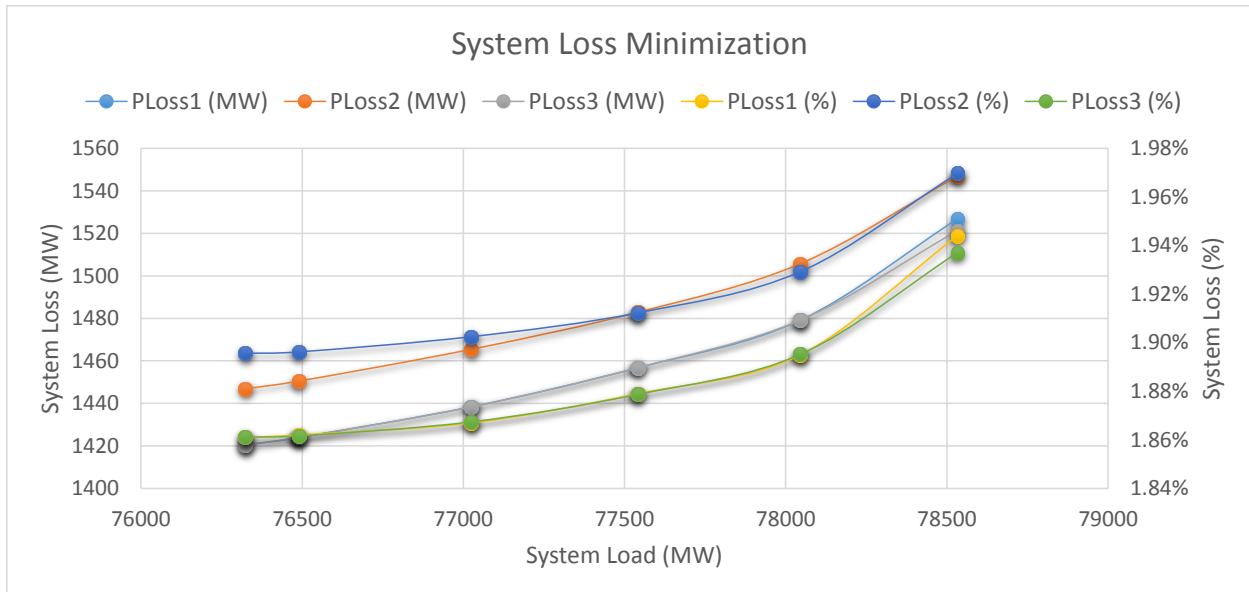


Figure 3-4: Post-contingency loss minimization under different loading conditions

The results on post-contingency production cost minimization are summarized in Table 3-9 and Figure 3-5. In the results,

- PCost1: the basecase OPF solution costs,
- PCost2: the post-contingency-558 OPF solution costs, and
- PCost3: the post-contingency-2909 OPF solution costs.

Similar observations can be drawn from the cost minimization results as from the above loss minimization results.

Table 3-9: Post-contingency cost minimization under different loading conditions

Case	Load (MW)	Ctg_558			Ctg_2909		
		PCost2 (\$/Hr)	Iters	Time (s)	PCost3 (\$/Hr)	Iters	Time (s)
1	76323.36	7582858.57	55	5.79	7582601.81	44	4.61
2	76489.11	7602631.16	66	6.95	7599915.84	42	4.40
3	77024.66	7662677.88	53	8.15	7659999.27	57	13.44
4	77541.53	7721382.9	40	4.25	7719793.49	55	5.92
5	78044.94	7777963.71	65	6.97	7775321.97	91	15.62
6	78532.81	7839068.25	55	8.36	7838036.41	78	8.40

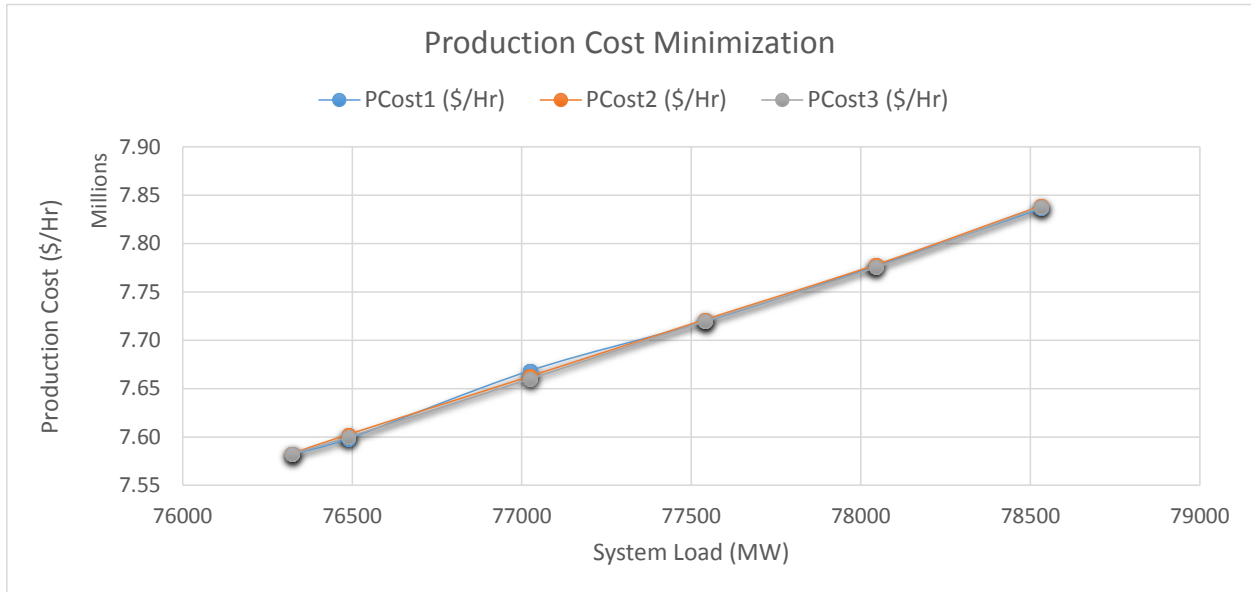


Figure 3-5: Post-contingency cost minimization under different loading conditions

### 3.4 Base-case + Individual Contingency Co-optimization

In this simulation, SuperOPF is used to co-optimize the base case system and individual worst contingency.

Table 3-10: Convergence for “basecase + single-contingency” co-optimization

Case	Load (MW)	IPM				SuperOPF
		Loss Minimization		Cost Minimization		
		Ctg_558	Ctg_2909	Ctg_558	Ctg_2909	
1	76323.36	Converged	Failed	Failed	Failed	Converged
2	76489.11	Converged	Failed	Failed	Failed	Converged
3	77024.66	Converged	Failed	Converged	Failed	Converged
4	77541.53	Converged	Failed	Failed	Failed	Converged
5	78044.94	Converged	Converged	Converged	Converged	Converged
6	78532.81	Failed	Converged	Failed	Failed	Converged

Table 3-10 summarizes the convergence for the “basecase + single-contingency” co-optimization under different loading conditions. It can be seen that conventional IPM

cannot converge for co-optimization under all loading conditions; more specifically, it failed to converge for 14 among 24 cases. In contrast, our SuperOPF solution method has successfully converged to the desired OPF solutions for all contingencies under all loading conditions.

Table 3-11: “Basecase + single-contingency” co-optimization for loss minimization

Case	Load (MW)	Basecase + Ctg_558			Basecase + Ctg_2909		
		P <sub>Loss2</sub> (MW)	Iters	Time (s)	P <sub>Loss3</sub> (MW)	Iters	Time (s)
1	76323.36	1435.87 (1.881%)	63	14.86	1435.57 (1.881%)	123	37.63
2	76489.11	1439.39 (1.882%)	146	34.89	1438.14 (1.880%)	189	53.72
3	77024.66	1454.05 (1.888%)	225	52.94	1454.58 (1.888%)	145	44.62
4	77541.53	1472.60 (1.900%)	228	55.06	1472.51 (1.899%)	61	24.22
5	78044.94	1494.63 (1.915%)	123	28.71	1494.91 (1.915%)	111	22.32
6	78532.81	1540.30 (1.961%)	227	64.66	1537.25 (1.957%)	92	21.69

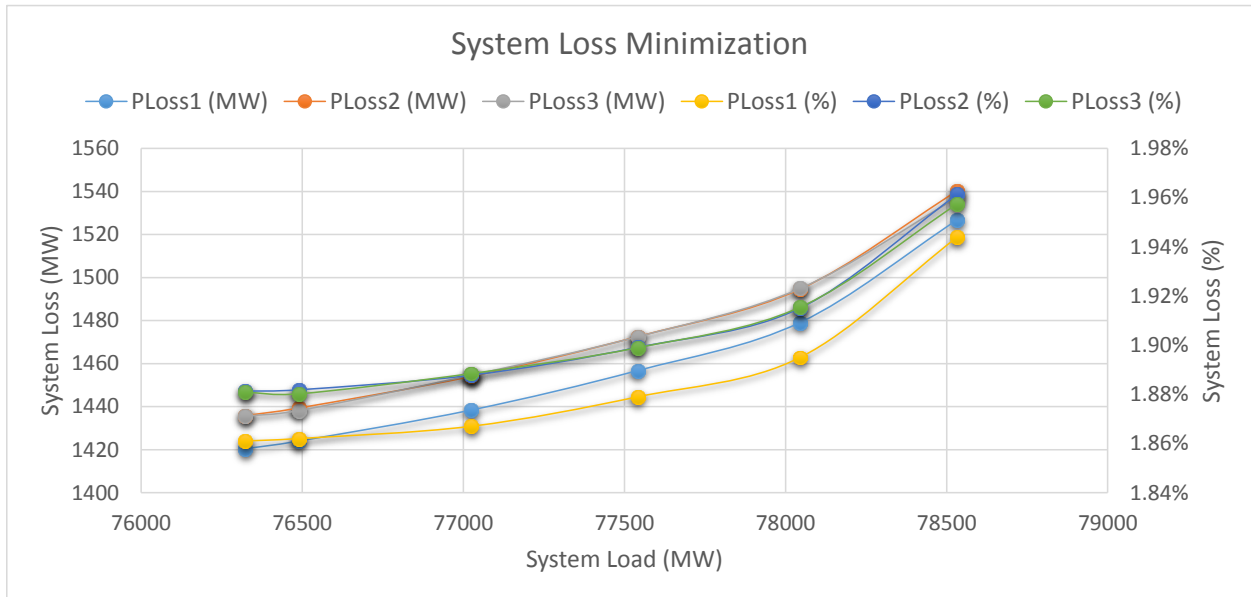


Figure 3-6: “Basecase + single-contingency” co-optimization for loss minimization

The results of co-optimization for power loss minimization are summarized in Table 3-11 and Figure 3-6. In the results,

- PLoss1: the basecase OPF solution losses,
- PLoss2: the “basecase + contingency-558” co-optimized OPF solution losses, and
- PLoss3: the “basecase + contingency-2909” co-optimized OPF solution losses.

Following observations can be drawn from the results:

- SuperOPF can robustly co-optimize the basecase system with worst contingency constraints under all feasible loading conditions, even though the contingencies are insecure.
- Since only one transmission line is taken out in the “N-1” contingencies, its impact on the resulted co-optimized system losses is also not significant. As shown in Table 3-11, the variations of the co-optimized OPF losses are about 1% with respect to the basecase OPF losses.
- The differences between different co-optimized system losses are less than that between post-contingency minimized system losses.
- Considering the optimization problem size (the number of optimization variables and the number of constraints) is roughly doubled for the co-optimization problem as compared to the basecase OPF problem, the computational time is also roughly doubled (per iteration).
- Due to the increased problem complexity, the computation tends to require more iterations to converge to the co-optimized OPF solutions.

Table 3-12: “Basecase + single-contingency” co-optimization for cost minimization

Case	Load (MW)	Basecase + Ctg_558			Basecase + Ctg_2909		
		PCost2 (\$/Hr)	Iters	Time (s)	PCost3 (\$/Hr)	Iters	Time (s)
1	76323.36	7714212.64	63	31.45	7714114.04	82	36.20
2	76489.11	7732790.70	61	20.70	7732559.20	105	42.17
3	77024.66	7798172.14	149	35.47	7793811.69	62	31.38
4	77541.53	7851769.17	51	29.49	7851824.31	71	33.91
5	78044.94	7910018.53	142	34.21	7910470.52	81	19.36
6	78532.81	7970888.42	264	81.39	7969248.91	181	60.20

The results on post-contingency production cost minimization are summarized in Table 3-12 and Figure 3-7. In the results,

- PCost1: the basecase OPF solution costs,
- PCost2: the “basecase + contingency-558” co-optimized OPF solution costs, and
- PCost3: the “basecase + contingency-2909” co-optimized OPF solution costs.

Similar observations can be drawn from the co-optimized cost minimization results as from the above co-optimized loss minimization results.

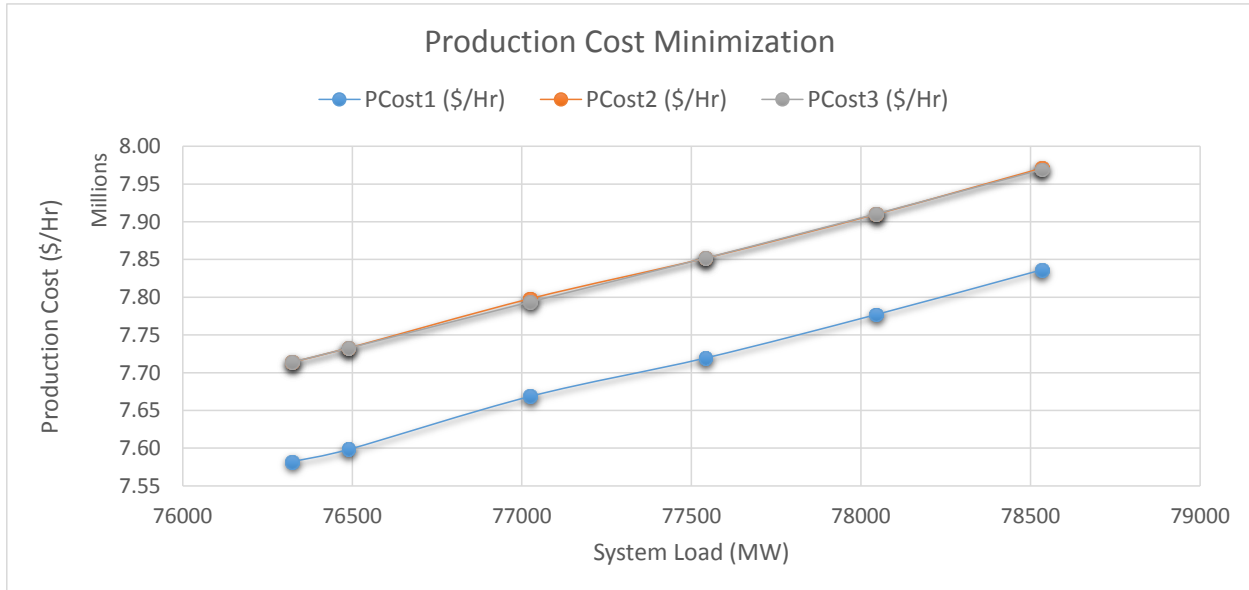


Figure 3-7: “Basecase + single-contingency” co-optimization for cost minimization

### 3.5 Base-case + All Contingency Co-optimization

In this simulation, SuperOPF is used to co-optimize the base case system and both worst contingencies.

Table 3-13 summarizes the convergence for the “basecase + all-contingency” co-optimization under different loading conditions. Similarly, it can be seen that conventional IPM cannot converge for co-optimization under all loading conditions; more specifically, it failed to converge for eight among 12 cases. In contrast, our SuperOPF solution method is able to converge to the desired solutions for all loading conditions, for both loss minimization and cost minimization.

Table 3-13: Convergence for “basecase + all-contingency” co-optimization

Case	Load (MW)	IPM		SuperOPF
		Loss Minimization	Cost Minimization	
1	76323.36	Failed	Failed	Converged
2	76489.11	Converged	Failed	Converged
3	77024.66	Failed	Failed	Converged
4	77541.53	Failed	Failed	Converged
5	78044.94	Converged	Converged	Converged
6	78532.81	Converged	Failed	Converged

The results of co-optimization for power loss minimization are summarized in Table 3-14. In the results,

- PLoss1 corresponds to the basecase OPF solution losses,
- PLoss2 for the “basecase + contingency-558” co-optimized OPF solution losses, and
- PLoss3 for the “basecase + contingency-2909” co-optimized OPF solution losses.

Following observations can be drawn from the results:

- SuperOPF can still robustly co-optimize the basecase system with worst contingency constraints under all feasible loading conditions, even though the contingencies are insecure.
- Since only one transmission line is taken out in the “N-1” contingencies, its impact on the resulted co-optimized system losses is also not significant. As shown in Table 3-14, the variations of the co-optimized OPF losses are about 1% with respect to the basecase OPF losses.
- The differences between different co-optimized system losses are less than that between post-contingency minimized system losses.
- Considering the optimization problem size (the number of optimization variables and the number of constraints) is roughly doubled for the co-optimization problem as compared to the basecase OPF problem, the computational time is also roughly doubled (per iteration).

- Due to the increased problem complexity, the computation tends to require more iterations to converge to the co-optimized OPF solutions.

Table 3-14: “Basecase + all-contingency” co-optimization

Case	Load (MW)	Loss Minimization			Cost Minimization		
		P <sub>Loss6</sub> (\$/Hr)	Iters	Time (s)	P <sub>Cost6</sub> (\$/Hr)	Iters	Time (s)
1	76323.36	1449.96	215	134.73	7714284.52	84	60.41
2	76489.11	1453.26	173	70.16	7732869.31	89	43.80
3	77024.66	1468.05	133	64.52	7793250.29	87	79.41
4	77541.53	1486.65	118	72.98	7851992.34	186	134.71
5	78044.94	1515.52	237	123.66	7910274.56	77	26.90
6	78532.81	1553.22	69	33.69	7970107.54	303	169.59

Finally, for a better comparison, the results are condensed in two Figures. More specifically, a condensed summary is provide in Figure 3-8 for the results on loss minimization for all involved simulations, where

- P<sub>Loss1</sub>: the basecase OPF solution losses,
- P<sub>Loss2</sub>: the post-contingency-558 OPF solution losses,
- P<sub>Loss3</sub>: the post-contingency-2909 OPF solution losses,
- P<sub>Loss4</sub>: the “basecase + contingency-558” co-optimized OPF solution losses,
- P<sub>Loss5</sub>: the “basecase + contingency-2909” co-optimized OPF solution losses, and
- P<sub>Loss6</sub>: the “basecase + all-contingency” co-optimized OPF solution losses.

Similarly, a condensed summary is provide in Figure 3-9 for the results on cost minimization for all involved simulations, where

- P<sub>Cost1</sub>: the basecase OPF solution costs,
- P<sub>Cost2</sub>: the post-contingency-558 OPF solution costs,
- P<sub>Cost3</sub>: the post-contingency-2909 OPF solution costs,
- P<sub>Cost4</sub>: the “basecase + contingency-558” co-optimized OPF solution costs,
- P<sub>Cost5</sub>: the “basecase + contingency-2909” co-optimized OPF solution costs, and
- P<sub>Cost6</sub>: the “basecase + all-contingency” co-optimized OPF solution costs.

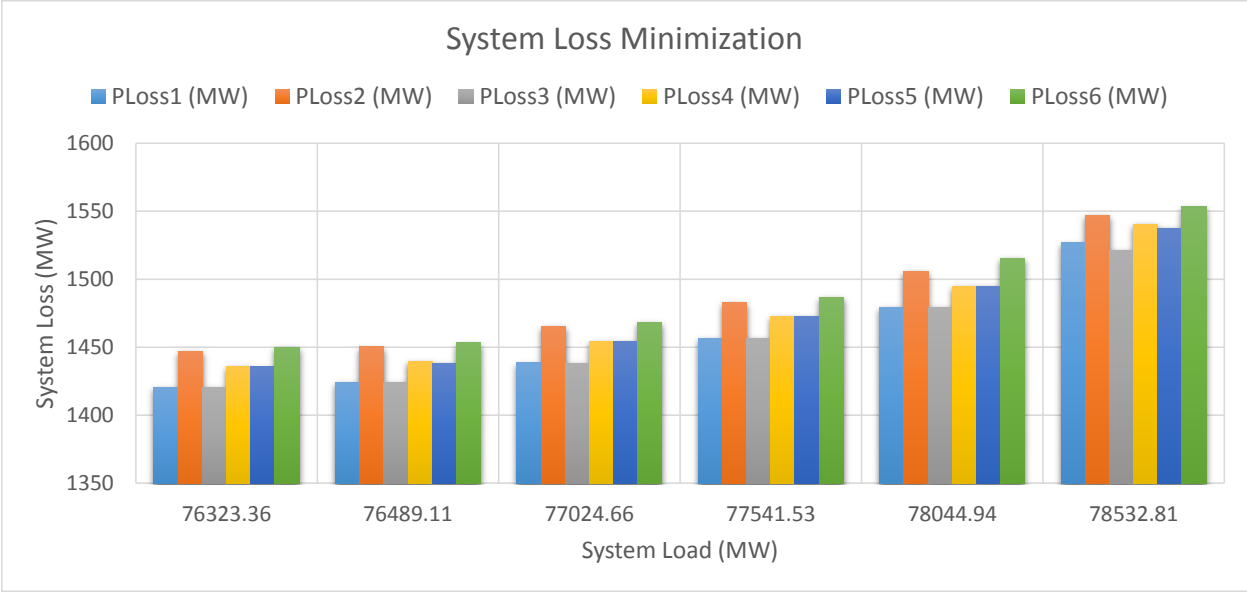


Figure 3-8: Summarized loss minimization results

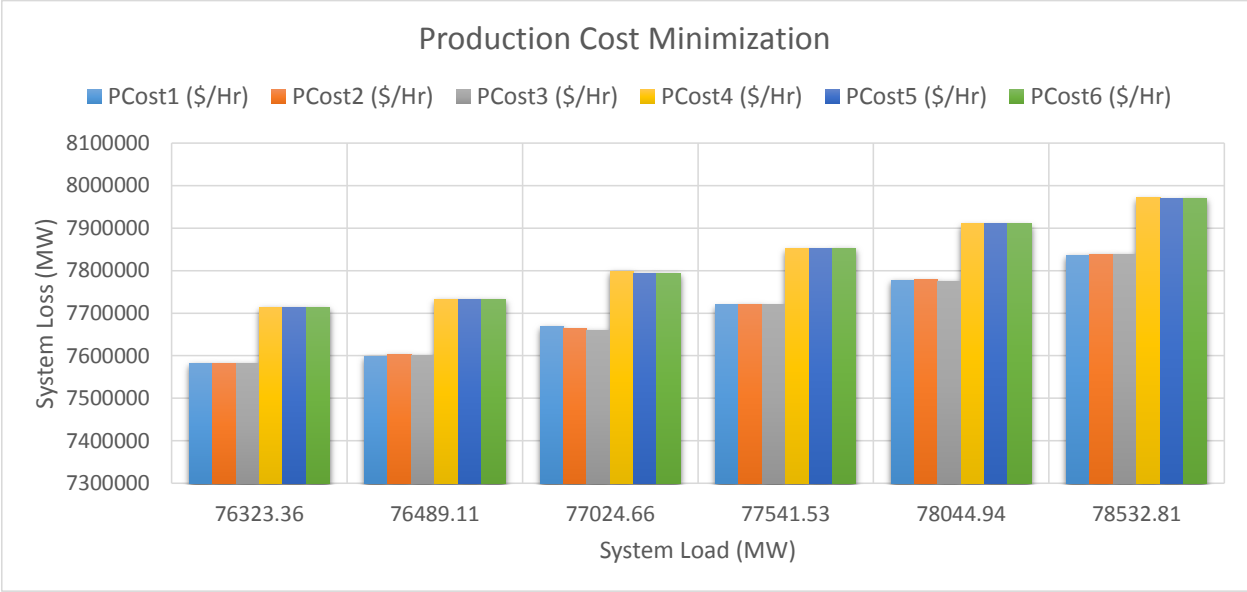


Figure 3-9: Summarized cost minimization results

## 4. Summary

In this report, a new dataset for SuperOPF computation is created. Based on this dataset, following simulations have been carried out:

- SuperOPF computation on the basecase and post-contingency systems, and
- SuperOPF co-optimization for “basecase + single contingency” and “basecase + all contingency”.

All simulations have been carried out for two OPF objectives, namely, system real power loss minimization and production cost minimization, and under different loading conditions.

The simulation results have shown that SuperOPF can robustly compute the OPF solutions for all the involved scenarios and under all feasible loading conditions, even though the post-contingency systems are insecure. Along with its comprehensive modeling capability, it is promising that SuperOPF can be a viable analysis tool for power industry.